# A LITERATURE SURVEY ON THE AERODYNAMIC PERFORMANCE OF DISTRIBUTED PROPULSION SYSTEMS

Doğa Çavlı[1], Ilgın Çolak[2], Merve Eşdur[3], Berkan Anılır[4], Tuğçe Kılcı[5], Hüseyin Metin Erikli[6], Hasan Mutlu[7], Serenay Tanrıverdi Yatkın[8], Fadile Yudum Çömez[9], Dilek Funda Kurtuluş[10]
METU
Ankara, Türkiye

Emre Kara[11]
Gaziantep University
Gaziantep, Türkiye

Erhan Solakoğlu[12]
Başkent University
Ankara, Türkiye

Mehmet Önder Efe[13]
Hacettepe University
Ankara, Türkiye

## ABSTRACT

*This paper presents a comprehensive literature survey on Distributed Propulsion (DP) systems, focusing on the aerodynamic integration of multiple propeller-wing configurations. Special attention is given to the influence of propeller positioning, spacing, and configuration types on overall aerodynamic performance. The study is conducted within the scope of a TÜBİTAK 1001 project, which aims to optimize DP systems through both experimental and numerical investigations. The findings from this survey aim to support the development of more efficient and innovative aircraft design methodologies using DP technologies.*

## INTRODUCTION

By distributing multiple smaller propulsion units across the airframe, along the wing or fuselage, Distributed Propulsion (DP) systems offer numerous potential advantages, including increased aerodynamic efficiency and better integration with electric and hybrid-electric power sources. These characteristics make DP systems particularly attractive for a wide range of applications, from urban air mobility (UAM) vehicles and electric vertical take-off and landing (eVTOL) aircraft to high-efficiency fixed-wing configurations. It currently becomes important to perform studies to understand the effect of the spanwise-distributed propellers along the wing

[1] M.Sc. Student in Aerospace Engineering, Email: doga.cavli@outlook.com
[2] Graduate Research Assistant in Aerospace Engineering Department, Email: cilgin@metu.edu.tr
[3] Graduate Research Assistant in Aerospace Engineering Department, Email: mesdur@metu.edu.tr
[4] Graduate Research Assistant in Aerospace Engineering Department, Email: anilir.berkan@metu.edu.tr
[5] Undergraduate Student in Aerospace Engineering, Email: tugce.kilci@metu.edu.tr
[6] M.Sc. Student in Aerospace Engineering, Email: metin.erikli@metu.edu.tr
[7] M.Sc. Student in Aerospace Engineering, Email: mutlu.hasan@metu.edu.tr
[8] M.Sc. Student in Aerospace Engineering, Email: serenaytnd@gmail.com
[9] Ph.D. Researcher RUZGEM, Email: yudumc@metu.edu.tr
[10] Full Professor in Aerospace Engineering Department, Email: kurtulus@metu.edu.tr
[11] Asst. Prof. in Aerospace Engineering Department, Email: emrekara@gantep.edu.tr
[12] Asst. Prof. in Mechanical Engineering Department, Email: erhansolakoglu@baskent.edu.tr
[13] Full Professor in Computer Engineering Department, Email: onderefe@gmail.com

on the aerodynamics of the designed aircraft systems [Fouda et al., 2019; Cakır et al., 2019; Fouda et al., 2022; Cigal et al., 2022; Minervine et al., 2022; Imran et al., 2023; Goli et al., 2023,2025; Lee et al., 2024].

The current paper aims to provide a comprehensive overview of the current state of the art in distributed propulsion systems. It will cover key findings from experimental and computational studies, explore different design strategies and configurations, and identify critical challenges and gaps in existing knowledge.

By synthesizing recent advancements and ongoing developments, the current 3-year TUBITAK 1001 project will focus on the optimization of Distributed Propulsion (DP) systems through a combination of experimental and numerical investigations, aiming to establish a comprehensive database to support the design of both fixed-wing and vertical take-off and landing (VTOL) platforms—whether manned or unmanned—and to address a critical need in the development of modern electric and hybrid aircraft. Given the rising interest in DP technologies for next-generation aviation, the outcomes of this research are expected to significantly influence ongoing global efforts and serve as a reference in the field.

The study will encompass the time-dependent flow simulations and wind tunnel experiments for four distinct propeller-wing configurations: a bare wing, a wing with a single propeller, a wing with two side-by-side propellers (Figure 1), and a wing with tandem-mounted propellers (one front, one rear). By varying Reynolds numbers, angles of attack, propeller diameters, and spacing, the effects on performance metrics such as lift, drag, and propeller-induced flow are systematically analyzed. It is intended to conduct flow simulations and experimental measurements at a wide range of Reynolds numbers ($1.25 \times 10^5 - 5.0 \times 10^5$) and angles of attack (0°-30°). The effects of propeller diameter and spacing on performance parameters will also be studied. These studies will also be conducted with both rectangular wing ($AR = 5$) and crescent wing [Raymer, 2025].

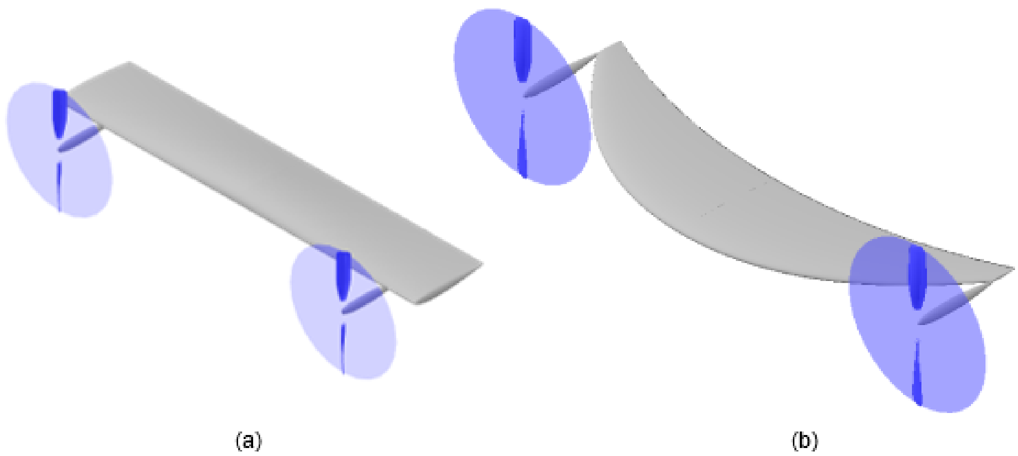


Figure 1*:* The two-propeller configurations a) rectangular wing b) crescent wing

## LITERATURE REVIEW

The 21st century's ever-increasing travel demands have raised awareness of energy and environmental issues related to aviation. Due to the limited supply of conventional petroleum fuel sources and the possible worldwide risks associated with emissions from conventional aircraft propulsion systems, the need for environmentally friendly aircraft technology solutions has now emerged as a major global concern [Kim et al., 2018]. The DEP (Distributed Electric Propulsion) structure aims to improve the aircraft's handling performance, emissions, acoustic noise, landing field length, and fuel efficiency. Also, to further reduce fuel use and increase efficiency, DEP can be more easily combined with BLI (Boundary Layer Ingestion) technology [Fard et al., 2022].

A dual-row propeller design was proposed by [Manzel, 1924] so that airplanes could take off without a runway. To make landings safer, Altieri added supplementary propellers in 1932. Griffith then switched out propellers for gas turbines in 1954, which allowed thrust vectoring, short take-off and landing (STOL), and increased fuel efficiency [Gohardani et al.,2011]. These early developments served as the basis for more recent Distributed Propulsion (DP) ideas, which have undergone substantial development. The literature review section is divided into five parts: experimental investigations, numerical investigations, multidisciplinary perspectives, validation and cross-comparison, and lastly, gaps and future research opportunities. Different aspects of the DP technology are analyzed, and the latest research is discussed.

**Experimental Investigations**

Experimental studies on distributed propulsion systems aim to understand the complex interactions occurring between the wing and the propellers. Researchers study the influences of various parameters on interactional dynamics and try different configurations to observe the variation of performance characteristics. As a relatively new area of research, including such complex aerodynamic interactions, many recent studies aim to provide data for distributed propulsion systems. This data is valuable for understanding the physics of various phenomena, validating computational methods, and improving the design of such systems. For easier comparison, the studies discussed in this section are summarized in Table 1.

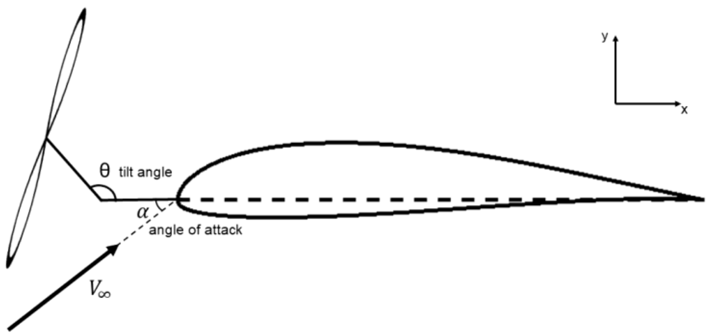


Figure 2: Airfoil Schematic

The effect of the propeller tilt angle (θ) (see Figure 2) on wing-propeller interactional aerodynamics is investigated through the wind tunnel measurements of a system consisting of a rectangular wing and a scaled propeller setup matching the XV-15 tiltrotor as described by [Srivathsan and Rauleder, 2024]. Their main purpose is to provide experimental data on flow field and pressure distributions, especially for the transition phase, which is equivalent to that from hover to cruise in a tiltrotor aircraft. The wing and propeller for which the characteristics are given in Table 1, are mounted on different support structures, maintaining 0.64m distance upstream and to the right laterally between wing spar and the support pole to prevent its wake to disrupt the flow over the wing. Flow fields were captured with stereoscopic particle image velocimetry (PIV), enabling a two-dimensional three-component (2D3C) measurement with cameras placed on the floor and the ceiling. Surface pressures were measured with high-resolution transducers at different spanwise locations on the wing. In the experiment, a single propeller is located at the midspan of the wing and the propeller tilt (nacelle) angle held constant for varying test parameters such as angle of attack $\alpha$ from −10° to 20°, the free-stream velocity $V_\infty$ from 0 to 30 m/s, propeller rotational speed $\Omega$ lower than 6000 rpm, and propeller tilt angle $\theta$ from 0° to 90°. Their study showed that for $\theta$ =45°, the velocity distribution in the propeller wake is affected by the wing circulation direction and wing angle of attack. Also, a recirculation region, most eminently observed for $\theta$ =90° and -10° angle of attack, is caused by the interaction between the wing boundary layer and the propeller slipstream. Wing boundary layer interactions lead to a thicker propeller wake for tilt angles between 60° and 90° near the upper surface.

[Leng et al., 2019] investigate the high-incidence conditions confronted by a propeller during the transition flight of a micro aerial vehicle through the measurements of forces and moments on the propellers at various advance ratios and blade pitch angles. Incidence angle $\alpha_p$, is defined as the angle between wind direction and the propeller axis of rotation. To simulate the variation of the incidence angle, propeller-motor system is mounted on a movable mast from the ceiling so that the whole system can rotate its vertical axis by 180° in both directions and thus the incidence angle can range between 0° to 180°. Several simplified propellers of a constant chord and NACA0012 blade section profile and of different pitch angles due to different blade tip angles $\beta_{tip}$ were tested at four different advance ratios. The freestream velocity and rotation speed are adjusted to obtain the desired advance ratio. For example, for $\beta_{tip}$ = 20°, advance ratios are 0.20, 0.45, 0.70, and 1.00 where corresponding $V_\infty$ values are 3, 6, 9, and 10 m/s. In the experiment, variation of aerodynamic forces and moments with advance ratio and incidence angle are observed for a high pitch $\beta_{tip}$ = 20° and a low pitch $\beta_{tip}$=10° propeller. Variations in thrust and torque coefficients, normal force coefficients, yaw moment coefficients, and pitching moment coefficients are analyzed with respect to advance ratio, blade pitch, and the rotational stall-delay effect. As a result, it is found that the yaw moment and normal force coefficients increase quasi-linearly while the thrust and torque coefficients increase non-linearly with increasing incidence angle. It is also observed that these effects are amplified for larger advance ratios and pitch angles. Pitching moment was detected as a secondary effect, showing minimal variation with changes in advance ratio or blade pitch angle.

[De Vries et al., 2021] indicates a gap in the literature regarding the interactions among propellers in forward flights and targets this gap in their experimental investigation. The system consists of three propellers installed side by side without a wing to observe the sole effect of adjacent propellers. The influence of one propeller on another diminishes rapidly with separation distance, thus, placing one propeller on each side of the middle propeller is sufficient to observe their interactions. Experiments are conducted for a nominal freestream velocity of $V_\infty$ = 30 m/s and blade Reynolds numbers $3.8 \times 10^4$ and $6.0 \times 10^4$ at 70% radius with a propeller blade pitch of 30° ± 0.05° at 70% of the blade radius for different configurations, including the isolated configuration, forward stagger, backward stagger and staired stagger configurations and a distributed configuration. The blade pitch angle is set to achieve maximum efficiency at a high thrust setting, and thus it is more aligned with take-off conditions than with cruise conditions. In this way, higher thrust and blade tip Mach number coefficients are achieved, making the interactions more easily distinguishable. In the experiment, advance ratios are varied in a range from 0.8 to 1.35 while angle of attack is chosen 0° and 5°. Both co-rotating and counter-rotating directions are tested. An ATI MINI-40E six-component force sensor is used to measure the forces exerted on the middle propeller. Furthermore, velocity distributions upstream and downstream of the propellers are measured using stereoscopic PIV. Additionally, total pressure distribution is measured in the vicinity of the propeller, providing insight into the non-uniform loading distribution on the propeller disc and further downstream regions, where slipstream deformation is observed. Moreover, to have a conception of the noise production microphone measurements are carried out. The main interaction phenomena is explained through a velocity field and slipstream characteristics analysis. Then, the influence of various operating conditions and design choices such as rotation direction, angle of attack, stagger, differential thrust, and relative phase angle is discussed. The main findings can be outlined as follows: Compared to the isolated configuration, distributed-propeller configuration has lower propeller thrust and efficiency for a given rotational speed; the efficiency of the middle propeller is observed to reduce by 1.5% due to interactions in the case of a thrust setting corresponding to the maximum efficiency. This efficiency drop is larger for the higher angles of attack and lower thrust settings, while independent of the rotation direction and relative blade phase angle. Local loading variations on the propeller disc up to 5-10% of the average disc loading are observed due to the velocities induced by the adjacent propeller slipstreams. Furthermore, it can be concluded from the results that the directivity pattern of the system can be altered by the active control of the relative blade phase angles.

High-lift configurations are also of interest, as [Oldeweme et al., 2022] aim to obtain high-fidelity experimental data on the positive effects of distributed propulsion on system performance in such configurations. They study the effect of various design parameters such as size, thrust, advance ratio, blade loading and local blade loading distribution, and design strategy. Regarding the coupling between propeller and wing, effects of relative horizontal and vertical propeller position to wing, spanwise propeller position, and inclination angle are examined. Finally, parameters related to the wing's high-lift performance such as flap setting and leading edge design are investigated. The system consists of a wing in high lift configuration with a 15.3% thick airfoil with 2% camber, a fowler flap, and three propulsion units placed on a different carrier. Propulsion units equipped with three types of blades specially designed by CIRA, namely A, B, C. Blade A has a tip diameter D = 0.6 m with a hub diameter $D_h$ = 0.1896 m and specifically designed for minimum induced losses (MIL), while blade B, having the same tip and hub diameters, is designed for a constant radial output velocity. Blade C with D = 0.4 m and $D_h$ = 0.1308 m are also designed for MIL. Three different propeller configurations are tested. In addition to the propeller configurations, advance ratio of 0.649 and 0.909; freestream velocity $V_\infty$ of 40 m/s and 55 m/s; angle of attack ranging from -10° to 22° , and propeller diameter D of 0.4 m and 0.6 m are among the experiment parameters. Pressure Sensitive Paint (PSP) is used on the top surface of the wing, and three dynamic pressure sensors are installed so that the temporal data of the swirl-induced angle of attack in the propeller wake can be obtained. The images provided through PSP help to visualize the time-averaged pressure distribution. according to various criteria such as minimum induced losses and constant radial output velocity. The experimental results provide a complete temporal mean state of the airfoil flow including flow patterns, laminar-turbulent transition and pressure distribution is covered owing to the selected measurement methods.

Moreover, since the propeller sets are designed and dimensioned differently but with the same thrust coefficients and blade tip speeds, comparable data for various advance ratios are obtained.

Table 1: Comparative summary of experimental investigations (configurations, system, method, and headline results)

| Study | Configuration & Focus | Wind Tunnel & Re | Wing/Propeller Characteristics | Experimental Method | Headline Result |
|---|---|---|---|---|---|
| [Leng et al. ,2019] | High-incidence conditions during transition flight | ISAE SaBRe low Re wind tunnel, close circuit, 1.2m × 0.8m test section.<br>Re at 75% $5.3 \times 10^4$, $4.7 \times 10^4$, $4.5 \times 10^4$, $3.5 \times 10^4$ | A constant chord and NACA0012 blade section profile<br>twist distribution β = tan−1 C r¯, (where C = tan $\beta_{tip}$ and r¯ is fractional radius) low pitch βtip = 10◦ and high pitch βtip = 20◦ | Force and moment measurements | Significant increase in aerodynamic forces and moments; and nonlinear increase in thrust and torque coefficients for increasing incidence angle<br>amplified for larger advance ratios and pitch angles<br>Pitching moment shows minimal variation with changes in advance ratio or blade pitch angle. |
| [de Vries et al., 2021] | Forward flight for various configurations (isolated,stagger,distributed) | Low speed, lowturbulence tunnel (LTT) at Delft University of Technology<br><br>Test section; 1.25 m x 1.8 m<br><br>Blade Reynolds number at 70% radius between $3.8 \times 10^4$ and $6.0 \times 10^4$ | Three "XPROP-S" propellers: six-bladed, steel radius of R = 101.6 mm | PIV, pressure measurements, load measurements | Efficiency of the middle propeller reduced by 1.5 % due to interactions<br>Local loading variations due to the velocities induced by the adjacent propeller slipstreams<br>directivity pattern of the system can be altered by the active control of the relative blade phase angles. |
| [Oldeweme et al., 2022] | High-lift configurations | Propulsion Test Facility (PTF) of the Institute of Jet Propulsion and Turbomachinery<br><br>Max. speed of M = 0.20<br>2.4 m x 2.4 m test section, turbulence level is Tu < 0.05 %<br>Operating conditions between Re = $2.1 \times 10^6$ and $2.9 \times 10^6$ | 15.3% thick, 2% cambered airfoil with a Fowler flap (CIRA/IRON Project).<br>Three propulsion units<br>Blade A: D = 0.6m $D_h$ = 0.1896m, MIL<br>Blade B: D = 0.6m Dh = 0.1896m<br>Blade C: D = 0.4m Dh = 0.1308m, MIL | Pressure measurements via Pressure Sensitive Paint (PSP) and dynamic pressure sensors | The full temporal mean state of flow patterns, laminar-turbulent transition and pressure distribution<br>Comparable data for various advance ratios |

| | | | | | |
|---|---|---|---|---|---|
| [Srivathsan and Rauleder, 2024] | Transition from hover to cruise | John J. Harper Wind Tunnel at the Georgia Institute of Technology<br><br>2.13m x 2.74m wind tunnel test section<br><br>Re = N/A | The wing is rectangular (NACA 0023, AR = 6.13, c = 0.25 m, b = 1.52 m, x = 0.3) and has an APC propeller (r = 0.19 m, pitch = 0.15 m). The prop–chord ratio is 2.38 and the prop–wing gap is 0.68c. | Stereoscopic PIV and pressure measurements with transducers | θ = 45° the velocity distribution in the propeller wake is affected by the wing circulation direction and wing α recirculation region at θ=90°<br>thicker propeller wake for 60◦ ≤ θ ≤ 90 near the wing upper surface due to BL interactions |

## Numerical Investigations

Recent numerical research on aero-propulsive integration focuses on two main approaches. The first is RANS (Reynolds-Averaged Navier Stokes) CFD (Computational Fluid Dynamics), where propulsors are represented with reduced-order models such as actuator disks calibrated using blade-element polars. The second is faster, lower-fidelity methods or code-to-code comparisons, which trade some accuracy for the ability to explore a larger range of designs. The comparative summary of numerical research is provided in Table 2.

In this context, cross-solver studies reveal both similarities and differences. [Russo et al., 2023] investigated three different CFD solvers, which are SU2, UZEN, and ANSYS Fluent, on a wing section with a forward-mounted tractor propeller at Re ≈ $1.7\times10^6$ and M ≈ 0.11. Additionally, the propeller is modeled as an actuator disk with a constant advance ratio of J = 0.63. The study showed that the three CFD solvers produced closely matching lift trends in power-on/off conditions, while the drag differed due to numerical diffusion and hub/disc implementations—underscoring the importance of discretization and propeller surrogates in predicting wake losses. SU2 predicts the lowest polar curve, while UZEN predicts the highest, resulting in flow solvers providing different drag coefficient estimates under power-off conditions, with a maximum discrepancy of $\Delta C_D$ = 50 counts. [Minervino et al., 2022] illustrate that at aircraft scale, Wingtip-Mounted Propellers (WTP) consistently yield cruise benefits by mitigating induced drag or, equivalently, increasing propulsive efficiency: a multi-fidelity study coupling RANS/actuator-disk with a vortex-lattice method reported up to ≈ 6% drag reduction in cruise (≈10% in climb) when tip propellers provided a share of total thrust and rotated against the wingtip vortex, with far-field breakdown confirming a reduction in reversible (induced) drag via span-efficiency gains.

[Schollenberger et al., 2025] investigated validation-oriented cruise simulations for WTP and spanwise DP utilizing an actuator disk propeller model, revealing WTP efficiency enhancements of several percent relative to wind-tunnel and in-flight data. The study also highlighted the sensitivity of turbulence models (SARC vs. SST) when reproducing cruise polars. A complementary regional-aircraft parametric study conducted by [Keller, 2021] determines aerodynamic and propeller performance using the TAU code, designed by the German Aerospace Center (DLR). In this study, 2 and 12 propeller configurations are used, and the actuator disk model is used to simulate the propellers. Moreover, the study found that DP alone is not automatically superior in cruise; however, combining WTP with thrust-sharing optimization and appropriate wing sizing reduced the required propulsive power by roughly 2.9–3.3% relative to a two-propulsor baseline. For small UAV scales, a sensitivity analysis conducted by Ma et al. in 2019 combining RANS with Kriging surrogates demonstrates that BLI can enhance aerodynamic and propulsive performance at moderate angles of attack ($\alpha \approx 2° – 6°$), while very low height position coefficients ($H_f \approx 0.05$) or larger setting angles (15°) may adversely affect propulsive efficiency and pitching moment—critical integration constraints for flying-wing designs.

To enable rapid exploration, NASA's X-57 effort assembled design-order toolchains (e.g., AVL/XFOIL-based aerodynamic build-ups linked to XROTOR with swirl inputs) and then cross-checked selected configurations with higher-fidelity CFD. The comparisons supported that the DEP wing should meet cruise targets while high-lift propulsors achieve low-speed objectives, clarifying analysis roles and limits at different design stages [Borer et al., 2017]. Furthermore, the rotor-wing interactions during conversion maneuvers were also investigated by [Tran & Yeo, 2023]. Tiltrotor conversion is modeled and analyzed using the comprehensive rotorcraft analysis code (RCAS) for the XV-15 aircraft. The study showed quasi-steady comprehensive analysis suffices across much of the envelope, but coupled CFD/CA (Comprehensive Analysis) is required to capture the onset/termination regions where wake interference and unsteady effects dominate. Finally, in ANSYS Fluent software, the aerodynamic study is performed using lifting line theory. The CFD results show that a wing with 65% of the area of the original wing has around 20% less drag. Aero-structural trades for commuter-class DEP highlight that aerodynamic gains must be balanced against structural load paths (e.g., higher spar shear for smaller wings), even as sizing studies suggest multi-percent fuel/energy reductions are achievable at the aircraft level [Hospodář et al., 2022].

The study of [Resende et al., 2022] focuses on two different types of DP, namely wingtip-mounted propellers and distributed propellers along the wingspan. Since there is comprehensive literature and well-established data of NASA's X-57 'Maxwell', it is selected as the benchmark for this study. The baseline configuration is the isolated wing, where in the second configuration only the wingtip-mounted propellers are on representing the cruise conditions (8000 ft & $Re = 2.7911 \times 10^6$) of the X-57. The third case in which the 12 high-lift propellers are deployed while the wingtip propellers remain operational simulates the typical landing conditions (sea level & $Re = 1.3126 \times 10^6$). For the analysis Open Vehicle Sketch Pad (OpenVSP) and VSPAERO code with an implementation of Lifting Surface Method are used. The propellers are modeled with the Actuator Disk model. The effects of propellers X position, propellers Z position and propellers pitch on the lift augmentation are investigated. The findings of the analysis confirm that further upstream positioning of the propellers enhances lift augmentation. However, the increase in lift coefficient $C_L$ observed in this study is lower than that reported in existing literature. Also, the negative pitch angles are found to have a positive effect on the effective α, thus improving the lift augmentation effect. Regarding the Z position, more significant lift augmentation is achieved when the rotor center has a close alignment with the wing. Also, more noticeable effect of Z position on lift is detected for lower advance ratios as it corresponds to lower rotational speed and thus less airflow is directed toward the wing.

Table 2: Comparative summary of numerical investigations (configurations, modeling, validation, and headline results)

| Study | Configuration & Focus | Re. | Propulsor Modeling | CFD Solver / Turbulence | Validation | Headline Result |
|---|---|---|---|---|---|---|
| [Borer et al., 2017] | NASA X-57 DEP: wingtip cruise propulsors + 12 high-lift propulsors | Cruise (8,000 ft, 150 kt); $4.34\times10^6$ m/c<br><br>High lift (0 ft, 58 kt); $2.04\times10^6$ m/c | Design-order (AVL/XFOIL + XROTOR with swirl) cross-checked with CFD | Multiple CFD solvers for pseudo-validation | Cross-code comparisons vs design-order predictions | DEP wing predicted to meet cruise; high-lift targets achieved with LE propulsors |
| [Ma et al., 2019] | Small-UAV DP with boundary-layer ingestion; mounting sensitivities | $7.19\times10^5$ (Cruise Conditions) | DP with BLI; surrogate-assisted (Kriging) RANS | RANS + surrogate modeling | In-study verification | BLI beneficial for α≈2°–6°; low mounting height/large setting angle penalize efficiency & Cm |
| [Keller, 2021] | Regional aircraft: DP sensitivities incl. WTP, thrust distribution, resizing | $12.4\times10^6$ (Cruise Conditions) | Actuator disk (2D-BEM-based) embedded in RANS | DLR TAU; RANS (SA-based with rotation correction) | Model-based parametric comparison | −2.9–3.3% required power vs 2-prop baseline when combining WTP + thrust sharing + resizing |
| [Resende et al., 2022] | Impact of wingtip-mounted propellers and distributed propellers along the wingspan | $2.7911\times10^6$ (cruise conditions)<br><br>$1.3126\times10^6$ (takeoff/landing conditions) | Actuator Disk model in VSPAERO | Mid-fidelity methodologies based on potential flow theory | In comparison to NASA X-57 reference data and advanced CFD, mesh convergence and drag integration calibration | Distributed propellers enhance $C_l$; wingtip propellers reduce generated drag |
| [Minervino et al., 2022] | Wing with inboard prop + WTP; cruise/climb drag breakdown | $16.6\times10^6$ (cruise conditions)<br><br>$12.8\times10^6$ (climb conditions) | Actuator disk (RANS) + VLM cross-check; far-field forces | SU2 / ZEN (RANS k-ω SST) + VLM | Cross-method comparison & mesh-sensitivity / far-field check | Up to ≈6% cruise and ≈10% climb drag reduction via WTP; reversible drag reduction confirmed |
| [Hospodář et al., 2022] | Commuter-class DEP aero-structural trade study | $3.5\times10^6$ (cruise conditions) | Integrated DEP sizing/loads (aero + structures) | RANS-informed methods; lifting-line aerodynamics | Internal consistency vs sizing targets | Multi-percent energy/fuel reduction feasible; structural load paths are limiting |
| [Russo et al., 2023] | Wing section + tractor propeller; | $1.7\times10^6$ (power-off and power- | Actuator disk with unified CT/CP radial inputs | SU2 / UZEN / ANSYS Fluent; steady RANS | Cross-solver comparison at | Good CL agreement; CD differences |

| | | | | | | |
|---|---|---|---|---|---|---|
| | code-to-code benchmark | on conditions) | | | $Re_\infty \approx 1.7\times10^6$, $M_\infty \approx 0.11$ | from numerical diffusion & hub treatment |
| [Tran & Yeo, 2023] | XV-15 conversion: quasi-steady CA vs coupled CFD/CA | N/A (fully turbulent) | Rotor/wing interaction captured with coupled CFD/CA | CFD/CA framework | Model-to-model comparison across conversion | Coupled CFD/CA needed at onset/termination for wake/interaction fidelity |
| [Schollenberger et al., 2025] | Cruise: wingtip propellers (WTP) and distributed propulsion (DP) vs isolated wing | $4.52\times10^5$; WTP<br>$5.22\times10^5$; DP | Actuator disk within RANS; trimmed cruise polars | DLR TAU ; SARC vs SST | Compared to wind-tunnel & in-flight polars | WTP/DP deliver cruise-efficiency gains; model choice matters for polar match |

## Multidisciplinary Perspectives on Distributed Propulsion

Researchers have taken a close look at DP systems, exploring how they affect aerodynamics, structural behavior, take-off and landings, and noise levels. Because DP system design encompasses numerous different areas, it is essential to understand how structural dynamics, noise, and efficiency are interconnected. Table 3 lists some key articles that showcase this work.

Table 3: Multidisciplinary Perspectives (source, subject, method(s) and result)

| Source | Subject | Method(s) | Result |
|---|---|---|---|
| [Nyugen et al., 2018] | Aeroelastic wing shaping control concept | 3D beam finite-element model | 2% performance gain |
| [Anderson, 2019] | Investigate the potential of distributed propulsion for suppressing wing flutter | Wind tunnel test and A 2-DOF numerical model, Theodorsen's unsteady aerodynamic theory | The system exhibited optimal control power at approximately 4 Hz |
| [Cusati et al., 2023] | Aerodynamic analyses in landing and take-off settings | High-fidelity numerical analyses with CFD-RANS solver | 27% reduction in take-off field length |
| [Turhan et al., 2024] | The effect of blade phase angle on noise attenuation | The aeroacoustic wind tunnel | Up to 24 dB of noise is reduced by a 90° phase angle between DEP propellers |
| [Keller, 2025] | Behavior under landing conditions of distributed propulsion | RANS simulations carried out with the DLR TAU code | Propeller count and thrust redistribution have a significant impact on lift performance during landing |
| [Simmons et al., 2025] | Aeroelastic damping of a wing-propeller system | Modeled in the Rotorcraft Comprehensive Analysis System | Wing flexibility and interactions between the propeller and wing minimize aeroelastic damping |

From an aeroelastic perspective, [Nyugen et al., 2018] examined wing shape control in distributed propulsion (DP) systems. The research showed that lift generated by thrust and wing flexibility can complement aerodynamic efficiency. Especially, when wing torsional stiffness is reduced by half and thrust is reconstructed to a more inboard and less outboard arrangement, a 2% improvement in performance is achieved. Additionally, [Simmons et al., 2025] discovered that wing flexibility and propeller–wing aerodynamic interactions can greatly reduce aeroelastic damping, with the greatest destabilizing effects occurring between propellers.

[Schubert et al., 2022] investigated the way distributed propulsion systems affect wings during gusts and landings and determined if existing wing designs require additional structural strengthening to accommodate these systems. But in distributed propulsion systems, [Keller, 2025] found that propeller count and thrust redistribution have a significant impact on lift during landing. Furthermore, DP systems influence aircraft take-off performance, with a maximum lift coefficient enhancement of up to 0.5 being seen at specific take-off speeds, potentially resulting in a 27% reduction in take-off field length compared to a conventional reference aircraft [Cusati et al, 2023].

Numerous studies have been investigating the impact of noise on DP. Controlling the relative phase angle of neighboring propellers can greatly lower the noise in a DEP system, according to [Turhan et al., 2024] study done on the impact of blade phase angle on noise attenuation in two adjacent electronically synchronized propellers.

The design of the system further influences the aerodynamic forces of the aircraft. Research done by [Schollenberger et al., 2024] showed that in cruise condition, the partial DP between 1 and 5 propellers per half-span is aerodynamically more efficient than a full span DP configuration. Besides, [Hospodář et al., 2022] investigated that the shear force that the spar must support increased when the wing's area, or construction height, was reduced. Therefore, to optimize distributed propulsion placement and wing structural design, aerodynamic efficiency must be balanced with the resulting structural load demands.

**Cross-Comparison**

The literature reviewed in preceding sections indicates numerous recent investigations on propeller-wing interaction employing experimental and computational methodologies independently. Also, some studies aim is to find the configuration that is most efficient for the DP systems. In this section, several studies using both methods and different configurations together for cross-comparison are discussed. Additionally, a summary of the papers covered in this section is provided in Table 4.

In one of the most recent studies, [Srivathsan et al., 2024] investigates the interactions in conversion from the edgewise to axial (cruise) flight based on unsteady aerodynamic load and pressure measurements and flow field measurements and a computational analysis. Their study covers axial condition where $\theta$ is zero, edgewise flight configuration where $\theta$ is 90° with a nonzero velocity, conversion condition where $\theta$ is between 15° and 75° , and hover condition where velocity is zero. The system consists of a finite, rectangular, untwisted wing which is an extrusion of an untwisted NACA 0023 symmetric airfoil having aspect ratio of 6.1270 (b = 1.5240 m, c = 0.2487 m) and a single propeller mounted on a different structure but close to the leading edge of the wing. The propeller is a two-bladed tractor propeller of radius r = 0.1905 m and with a fixed propeller pitch of 0.1525 m manufactured by APC. In the experiment, stereoscopic PIV is used at the streamwise location of the wing for two-dimensional three-component (2D3C) measurements. Also, unsteady wing surface pressure measurements are obtained through pressure scanners along the chord at several span wise locations.

Computational analysis employs the SAM Cart off-body Cartesian solver for four different cases based on angle of attack of the wing, tilt angle of the propeller, test section in the wind tunnel and free air simulation. Three types of meshes are used in the computational domain: FUN3D for tunnel, OVERFLOW for wing and SAMCart meshes filled the gaps between the unstructured and structured component meshes. It is observed both experimentally and computationally that significant amount of thrust and lift is induced by the propeller at cruise conditions where θ is zero, decreasing for high free stream velocity values. In the conversion conditions in which θ is between 15° and 75°, wing drag increases up to θ =45° then starts to decrease while the lift manifests the opposite behavior. Also, as θ increases, propeller thrust is increased. In the edgewise flight conditions where θ is 90°, propeller wake skew angles are crucially larger for the retreating sides compared to the advancing sides. For this condition, substantial interaction between the propeller wake and the wing on the retreating side is predicted by computational simulation while this is not observed in the experiments. This difference may be a result of the dissipation between near body meshes, or higher propeller thrust predicted computationally, or a combination of the two effects. Furthermore, advancing side wake experiences greater turbulent kinetic energies than the retreating side and thus, highly unsteady positive pressures on the upper surface of the wing behind the mid-chord is observed.

Following this work, same group of researchers conducted another study which investigates the interactions in a model-scale generic tractor proprotor–wing system at different proprotor tilt angles during the conversion maneuver in [Sridhar et al., 2025]. They use the data from the experiment to validate their computational method. CFD simulations are executed using CREATE™-AV Helios which is a high-fidelity rotorcraft simulation tool employing a multi-grid, multi-solver paradigm. Pointwise 2022.2.2 and Chimera Grid Tools are used for the generation of near-body structured grids. Resolution of the off-body computational domain is conducted by highly-parallelizable Cartesian block solver SAMCart is used. For the analysis of the conversion maneuver freestream velocity $V_\infty$ of 10 m/s, wing angle of attack of 0° rotational speed Ω of 7000 rpm are chosen as fixed variables where rotor tilt angle θ take the values of 0° to 90°. The proprotor thrust was trimmed to the experimental thrust loads using blade collective modulation for better comparison.

The comparison of experimental and computational analysis showed that the CFD simulations are mostly parallel to the experimental findings during the conversion maneuver. Furthermore, trends in wing lift and pitching moment coefficients are represented precisely although the wing download in the edgewise flight is overpredicted and drag coefficient is underpredicted. Regarding the complex aerodynamic interactions, researchers find out that the primary interactions in the axial flight occur close to the leading-edge stagnation region and at the trailing edge. Also, at low tilt angles in the conversion maneuver (15° ≤ θ ≤ 30°), the main reason for the interactions is detected as the flow separation at trailing edge on the lower surface of the wing. At higher angles (45° ≤ θ ≤ 60°), primary interactions occur at the leading-edge stagnation region. On the other hand, when the proprotor proceed to the edgewise flight (75° ≤ θ ≤ 90°), the only region in which the interactions take place is the wing upper surface.

[Lei and Zhao, 2023] studied the interactions in the pusher configuration of DEP systems using a four-propeller setup where the propellers are equally distributed along the rear wing. Each adjacent propeller rotates in opposite directions to its neighbor—for a four-propeller configuration, the rotation sequence is counterclockwise (CCW), clockwise (CW), counterclockwise, and clockwise. Propellers are mounted on a support pole which is parallel to the rear wing. The wing has NACA4415 airfoil through the whole span of 300 mm and the chord length is 150 mm. Propellers have 4 blades with 76.2 mm radius and 76.2 mm pitch. For the experiment, free stream velocity $V_\infty$ is set to 18 m/s and wing Reynolds number is 180,000. Rotational speed of the propellers is fixed to 18,000 rpm. Force sensors are used to find out the distribution of $C_l$ and $C_d$ for different rotor locations. Then, the results are compared with the baseline case which is the isolated wing. Also, numerical simulations are performed in FLUENT. Analysis of the external flow field is carried out using RANS model. Finite volume method is selected to discretize the differential equations and $k-\omega$ turbulence model is preferred due to low Reynolds number. For the pressure correction and interpolation, SIMPLE (Semi Implicit Method for Pressure-Linked Equations) algorithm is employed. For the interaction between the rotating and stationary regions, sliding grid is used and multiple reference frame (MRF) method is utilized for the initial condition for the slip mesh transient calculation. To investigate the increased lift at higher angles of attack, the velocity distribution at the 43% span section of the pusher configuration was chosen. The simulations were conducted with $\alpha$ varying between 20° and 30°. Pressure contours and vorticity distributions are obtained for different propeller locations and angle of attack values within this range. As a result of the analysis, in the pusher configuration, the propeller was affected by the wing's blocking effect and the wake generated at the wing's trailing edge and this interaction substantially increased the lift. Moreover, it is observed that the effect of the propeller is not remarkable for angles of attack lower than 16° but the lift coefficient is significantly greater than the baseline and lift of the system can be increased up to 73–87% without any decrease in L/D. The wing in the pusher configuration stalls at 16° angle of attack but when the pusher props are placed above the wing chord line, a delay in stall is observed. Drag coefficient is also increased particularly for the DEP with a smaller horizontal distance between the propeller and the trailing edge of the wing.

The study of [Zhang et al., 2023] is based on a hazardous a non-command nose-up occurred in the flight tests of an unmanned air vehicle (UAV) with Electric Ducted Fans (EDF) when the pilot slows down to land the aircraft. To understand this phenomenon, aerodynamic-propulsion coupling characteristics of the tandem wing DEP UAV is investigated using DEP demonstrator with 24 high-lift EDFs distributed along the trailing edge of a wing of 345 mm chord and 867 mm span, having NACA 4415 airfoil with a deflectable power unit. The focus is the effect of throttle and propulsion installation angle of EDFs on the aerodynamic performance for different $\alpha$. Experiments are carried out in a low-speed wind tunnel with a turbulence intensity Tu < 0.2% for all operating speeds, at Northwestern Polytechnical University. Upstream airspeed, angle of attack, throttle and the deflection angle of the EDF-mounted surface ($\delta_T$) is measured. For the calculation of three-axels force and moment coefficients, a 6-component force balance is utilized. Different lift-augmentation power conditions are compared with the clean configuration for the conditions of 15-25 m/s freestream flow and -4° to 6° angles of attack. For example, at a freestream velocity of $V_\infty$= 0 m/s, tests were conducted for deflection angles (δ) of 0°, 15°, and 30°, and α of – 4°, 2°, and 16°, across a throttle range of 0% to 100%. Also, at a freestream velocity of $V_\infty$ = 20 m/s, tests were performed at $\alpha$ of 0˚, 4˚, 16˚ with the δ fixed at 0°. Also, a CFD analysis is conducted and verified through the experiments. An in-house Navier Stokes code which employs a SIMPLE algorithm for the pressure-velocity coupled equation is used as the flow solver. Turbulence modeling is carried out by Spalart-Allmaras (S-A) model. The rotor disc method is preferred to simulate the effect of EDF on the wing performance as rapidly as possible. Unstructured grid is chosen to generate mesh more easily for the complex geometry of multiple EDFs on the wing.

With the analysis throttle change effect on aerodynamic performance is observed and the influence of EDF installation surface's deflection angle is examined. It is concluded that the experiment is verified the effect of BLI; i.e., EDFs produce lift and reduce drag at the same time due to the benefit of BLI at low speeds. For the $\alpha$ = 4˚, L/D can be increased from 7.2 to 21.57 and at $\alpha$ = 16° maximum $C_L$ can be increased from 0.836 to 1.429. Also, $C_D$ is significantly raised due to the additional structure of EDFs. This explains the non-command nose-up phenomenon occurred in the tests as the decrease in throttle in landing leads to an increased drag and reduced lift. Also, with δ = 30˚, maximum $C_L$ can be increased to 2.28 and the $C_D$ increment caused by the thrust device at a small angle of attack can be extinguished with the deflection of the surface. Regarding the CFD results, calculated lift shows good agreement with the experimental data. However, while the trend is well predicted for drag, its quantitative accuracy is limited.

Table 4: Comparative summary of Cross-Comparison investigations (configurations, system, CFD solver, experimental method, and headline results)

| Study | Configuration & Focus | Wind Tunnel & Re | Wing Propeller Characteristics | CFD Solver / Turbulence | Experimental Method | Headline Result |
|---|---|---|---|---|---|---|
| [Lei and Zhao, 2023] | Pusher configuration | Re=180,000 | Four-propellers of 4 blades with 76.2 mm radius and 76.2mm pitch<br><br>Wing of NACA4415 profile b=300 mm c=150mm | Force measurements | FLUENT is used for simulation. RANS model for external flow and $k-\omega$ Turbulence Model | Propeller can increase lift by 73–87% without lowering L/D, although it has little effect for $\alpha$ < 16°. Placing pusher props above the wing delays stall, which happens at $\alpha$=16°. |
| [Zhang et al., 2023] | Pusher configuration a non-command nose-up occurred in landing | Low-speed wind tunnel at Northwestern Polytechnical University. | 24 high-lift EDFs fitted at rear wing | Upstream airspeed, $\alpha$, throttle the deflection angle, force and moment measurements | In-house Navier Stokes code Spalart-Allmaras turbulence model | Experiment verified the effect of boundary layer ingestion (BLI). Deflection angles |

| | | | | | | |
|---|---|---|---|---|---|---|
| | | | | | | improve the lift. |
| [Srivathsan et al., 2024] | Conversion from edgewise to cruise | John J.Harper Memorial wind tunnel at the Georgia Institute of Technology | Untwisted wing with constant NACA 0023 profile, AR=6.127 Two-bladed tractor propeller of r=0.1905m fixed pitch of 0.1525m | PIV, pressure measurements, load measurements | SAM Cart off-body Cartesian solver Spalart-Allmaras model with Delayed-Detached Eddy Simulation (SA-DDES) | θ=0°: produces lift and thrust. 15°–75°: At 45°, drag peaks, lift falls, and then rises. θ=90°: increased wake skew and benefits of positive pressure |
| [Sridhar et al., 2025] | Conversion maneuver | John J. Harper Memorial wind tunnel at the Georgia Institute of Technology | Untwisted wing with constant NACA 0023 profile, AR=6.127 Two-bladed tractor propeller of r=0.1905m fixed pitch of 0.1525m | PIV, pressure measurements, load measurements | CREATE™-AV Helios high-fidelity URANS approach | Experimental results and CFD concur that interactions occur at the leading and trailing edges in axial flight and exclusively on the upper surface in edgewise (75°–90°) flight. |

**Gaps and Future Research Opportunities**

Regardless of significant advances in the understanding of the aerodynamic performance of DP and DEP systems, some significant research gaps still exist. Various experiments have shown promising benefits such as BLI, lift enhancement using blown air, which means boosting the lift by propellant slipstreams that accelerate airflow and delay the boundary layer separation, and improved propulsive efficiency [Amir et al., 2011; Keller, 2021; Cusati et al., 2023]. Although extensive studies show benefits from BLI and blown lift, these observations frequently come from limited test cases or configurations; thus, several comparative and CFD studies suggest additional validation is necessary before these benefits can be assumed to be generally applicable over all flight regimes [Borer et al., 2017; Qiao et al., 2024]. Likewise, there are still relatively few studies that comprehensively understand the unstable aerodynamic phenomena occurring during takeoff, landing, or tilt-rotor transitions. [Sridhar et al., 2025; Tran & Yeo, 2023].

CFD has been used heavily to study wing–propeller and propeller–propeller interactions [Qiao et al., 2024; Russo et al., 2023; Walvekar & Chakravarthy, 2023]. Wind tunnel testing [Srivathsan et al., 2024; Minervino et al., 2022] has successfully captured some aerodynamic phenomena, including wake-wing interactions; however, additional large-scale and high-speed tests are needed to replicate actual flight conditions more accurately. This is particularly necessary for high-lift configurations and high angles of attack, when propeller effects can significantly contribute to stall and lift generation.

Another unexplored area is aerodynamic optimization of propeller placement, phasing, and direction of rotation for better performance throughout the flight envelope. [Minervino et al., 2022] and [Keller, 2025] demonstrated that strategically positioning propellers, especially at wingtips or close to the wing leading edge, have the potential to reduce induced drag and delay flow separation, leading to measurable lift and overall efficiency gains. Besides, [de Vries et al., 2021] and [Schollenberger et al., 2024] demonstrated that adjusting propeller spacing and alignment can alter wake interaction patterns, influencing lift augmentation and propulsive efficiency. Most of these investigations, however, focus on a limited range of operating conditions, frequently steady forward flights without adequately considering off-design situations like takeoff, landing, or extreme crosswind operations.

Future research on DP system design must combine high-fidelity CFD with controlled experimental testing to elucidate the aerodynamic effects of propeller placement, phasing, and rotation over a range of flight conditions, thereby enabling optimization strategies that balance lift, drag, thrust efficiency, and stability for conventional and unconventional configurations. These efforts are essential to translate the aerodynamic benefits of dispersed propulsion into reliable, certifiable aircraft designs.

## CONCLUSION

A detailed review of the literature about Distributed Propulsion systems in terms of computational, experimental, cross-comparative and interdisciplinary studies is presented in this paper. It is intended to gather comprehensive insights from the most recent studies to support the TUBITAK 1001 project, which aims to optimize DP systems through both experimental and numerical investigations.

As demonstrated in the studies, DP systems involve complex aerodynamic interactions between the wing and the propellers and among the propellers themselves, which in turn affect the overall performance characteristics of the systems. Both pusher and tractor configurations performing various maneuvers and operating conditions including conversion, transition, cruise, forward flight and landing are examined elaborately. The diversity of these conditions necessitates a carefully tailored computational analysis. The intricacy of the flow field characterized by interactions among different slipstreams, wakes and boundary layers makes experimental investigations inevitable for understanding various physical phenomena and for validating the computational method.

This relatively new and rapidly evolving research area still contains significant gaps in literature and thus offers many future research opportunities. A substantial amount of data is needed to gain a deeper comprehension of the unstable aerodynamic phenomena occurring during takeoff, landing, or tilt-rotor transitions. Also, additional large-scale and high-speed tests are required to more accurately represent actual flight conditions. Optimization of propeller placement, phasing, and direction of rotation for better performance remain insufficiently explored.

**Acknowledgement**

This study was supported by Scientific and Technological Research Council of Türkiye (TUBITAK) under the Grant Number 125M095. The authors thank to TUBITAK for their support.

## References

Amir S. Gohardani, Georgios Doulgeris, Riti Sing. Challenges of future aircraft propulsion: A review of distributed propulsion technology and its potential application for the all-electric commercial aircraft, Progress in Aerospace Sciences, Volume 47, Issue 5, 2011, Pages 369-391, ISSN 0376-0421, https://doi.org/10.1016/j.paerosci.2010.09.001.

Anderson, C. (2019). Numerical and Experimental Investigation of Wing Flutter Suppression via Distributed Propulsion. Oregon State University.

Borer, N. K., Derlaga, J. M., Deere, K. A., Carter, M. B., Viken, S., Patterson, M. D., Litherland, B., & Stoll, A. (2017). Comparison of aero-propulsive performance predictions for distributed propulsion configurations. 55th AIAA Aerospace Sciences Meeting. https://doi.org/10.2514/6.2017-0209

Chinwicharnam, K., & Thipyopas, C. (2016). Comparison of wing–propeller interaction in tractor and pusher configuration. International Journal of Micro Air Vehicles, 8(1), 3–20. https://doi.org/10.1177/1756829316638206

Cigal, N, Naeem, N., Ratei P., Kilkis S., Prakasha P. S., Kurtulus D.F., Nagel B. Sensitivity Analysis for Aerial Wildfire Fighting Tactics with Heterogeneous Fleet via System of Systems Simulation Framework, Deutscher Luft- und Raumfahrtkongress 2022, DLRK 2022, 27-29 September 2022, Dresden, Germany.

Cusati, V., Corcione, S., Nicolosi, F., & Zhang, Q. (2023). Improvement of take-off performance for an electric commuter aircraft due to distributed electric propulsion. Aerospace, 10(3), 276. https://doi.org/10.3390/aerospace10030276

De Vries, R., van Arnhem, N., Sinnige, T., Vos, R., & Veldhuis, L. L. M. (2021). Aerodynamic interaction between propellers of a distributed-propulsion system in forward flight. Aerospace Science and Technology, 118, 107009. https://doi.org/10.1016/j.ast.2021.107009

Fouda M, Haq R., Naeem H.N., Saeed MA, Wanyonyi S. N., Cigal N, Beker C., Yayla M., Kurtulus D.F. (2019). Design Methodologies of a Distributed Propulsion Aircraft, AIAC-2019-057, 10th Ankara International Aerospace Conference, 18-20 September 2019, AIAC-2019-057, Ankara, ISBN: 978-975-429-393-7.

Fouda, M., Adler, E. J., Bussemaker, J.H., Martins J.R.R.A., Kurtulus, D.F., Boggero L., Nagel B. (2022). AUTOMATED HYBRID PROPULSION MODEL CONSTRUCTION FOR CONCEPTUAL AIRCRAFT DESIGN AND OPTIMIZATION, ICAS Paper 2022_0593, 33rd Congress of the international Council of the Aeronautical Sciences, Stockholm, Sweden, 4-9 September 2022.

Goli, S., Kurtulus, D.F, Alhems, L. M., Memon, A.M., Imran, I.H., Experimental study on efficient propulsion system for multicopter UAV design applications (2023), Results in Engineering, Vol.20, 101555, 10.1016/j.rineng.2023.101555 , pp1-18.

Goli, S.; Kurtuluş, D. F; Waqar, M.; Imran, I.H.; Alhems, L.M; Kouser, T.; Memon, A. M. (2025) Artificial neural network for the evaluation of electric propulsion system in unmanned aerial vehicles, Neural Computing and Applications.

Hospodář, P., Klesa, J., Demovič, D., & Žižkovský, N. (2022). Aerodynamic and structural aspects of a distributed propulsion system for commuter airplane. Aerospace, 9(11), 712. https://doi.org/10.3390/aerospace9110712

Hyun D. Kim, Aaron T. Perry and Phillip J. Ansell, "A Review of Distributed Electric Propulsion Concepts for Air Vehicle Technology", Jul 2018. AIAA/IEEE Electric Aircraft Technologies Symposium. https://doi.org/10.2514/6.2018-4998

Imran, I.H., Memon, A.M., Kurtulus, D.F, Goli, S., Alhems, L. M. (2023) Extended Sliding Mode Control Scheme for a VTOL UAV with Time-Varying Disturbances, 2023 AIAA Aviation Forum, 12-16 June 2023, San Diego, CA, DOI: 10.2514/6.2023-4461

Keller, D. (2021). Towards higher aerodynamic efficiency of propeller-driven aircraft with distributed propulsion. CEAS Aeronautical Journal, 12(4), 777–791. https://doi.org/10.1007/s13272-021-00535-5

Keller, D. (2025). Numerical study on lift augmentation via distributed propulsion for a propeller-driven regional transport aircraft in landing configuration. CEAS Aeronautical Journal. https://doi.org/10.1007/s13272-025-00863-w

Lei, Y., & Zhao, X. (2023). Aerodynamic performance assessment of distributed electric propulsion after the wing trailing edge. Applied Sciences, 14(1), 280. https://doi.org/10.3390/app14010280

Leng, Y., Jardin, T., Bronz, M., & Moschetta, J.-M. (2019). Experimental analysis of propeller forces and moments at high angle of incidence. AIAA Scitech 2019 Forum. https://doi.org/10.2514/6.2019-1331

M. T. Fard, J. He, H. Huang and Y. Cao, "Aircraft Distributed Electric Propulsion Technologies—A Review," December 2022. IEEE Transactions on Transportation Electrification, vol. 8, no. 4, pp. 4067-4090, Dec. 2022, DOI: 10.1109/TTE.2022.3197332.

Ma, Y., Zhang, W., Zhang, Y., Li, K., & Wang, Y. (2019). Effects of distributed propulsion crucial variables on aerodynamic and propulsive performance of small UAV. Lecture Notes in Electrical Engineering, 1535–1550. https://doi.org/10.1007/978-981-13-3305-7_123

Minervino, M., Andreutti, G., Russo, L., & Tognaccini, R. (2022). Drag reduction by wingtip-mounted propellers in distributed propulsion configurations. Fluids, 7(7), 212. https://doi.org/10.3390/fluids7070212

Nguyen, N. T., Reynolds, K., Ting, E., & Nguyen, N. (2018). Distributed propulsion aircraft with aeroelastic wing shaping control for improved aerodynamic efficiency. Journal of Aircraft, 55(3), 1122–1140. https://doi.org/10.2514/1.c034448

Oldeweme J., Lindner T., Scholz P., Friedrichs J. (2022). Experiment Design for a Distributed Propulsion Configuration at High Lift. Deutscher Luft- und Raumfahrtkongress. DOI: 10.25967/570125

Qiao, G., Zhang, T., & Barakos, G. N. (2024). Numerical simulation of distributed propulsion systems using CFD. Aerospace Science and Technology, 147, 109011. https://doi.org/10.1016/j.ast.2024.109011

Resende, G., Malatesta, V., Savio, M., & Castro, B. (2022). Study of effects on the wing's aerodynamic characteristic due to distributed propulsion over wingspan. International Council of the Aeronautical Sciences.

Russo, O., Aprovitola, A., de Rosa, D., Pezzella, G., & Viviani, A. (2023). Computational fluid dynamics analyses of a wing with distributed electric propulsion. Aerospace, 10(1), 64. https://doi.org/10.3390/aerospace10010064

Schollenberger, M., Firnhaber Beckers, M., Lutz, T., Krämer, E., Bergmann, D., Denzel, J., Strohmayer, A., Pfeifle, O., & Fichter, W. (2025). Cruise flight simulation of distributed propulsion and wingtip-mounted propeller aircraft and their validation with in-flight measurement data. CEAS Aeronautical Journal. https://doi.org/10.1007/s13272-025-00869-4

Schollenberger, Michael, Kirsch, B., Lutz, T., Krämer, E., & Friedrichs, J. (2024). Aerodynamic interactions between distributed propellers and the wing of an electric commuter aircraft at cruise conditions. CEAS Aeronautical Journal, 15(2), 255–267. https://doi.org/10.1007/s13272-023-00706-6

Schubert, M., Dafnis, A., & Schröder, K.-U. (2023). Gust and landing impacts as critical load cases for wings with distributed propulsion. Journal of Physics: Conference Series, 2526(1), 012039. https://doi.org/10.1088/1742-6596/2526/1/012039

Simmons, G., Riso, C., Cesnik, C., & Chang, J. (2025). Influence of wing-propeller aerodynamic interactions on aeroelastic damping. Proceedings of the Vertical Flight Society 81st Annual Forum and Technology Display, 1–13. https://doi.org/10.4050/f-0081-2025-208

Sridhar, P., Srivathsan, S., Rauleder, J., & Smith, M. J. (2025). Physics of the interactional proprotor-wing aerodynamics during the Tiltrotor Conversion Maneuver. Proceedings of the Vertical Flight Society 81st Annual Forum and Technology Display, 1–21. https://doi.org/10.4050/f-0081-2025-271

Srivathsan S. and Rauleder J. Wind Tunnel Measurements on the Effect of Propeller Tilt on Propeller-Wing Interactional. (2024). *AIAA Aviation Forum and ASCEND Co-Located Conference Proceedings*. https://doi.org/10.2514/MAVAS24;article:article:10.2514/6.2024-4146;requestedJournal:journal:6

Srivathsan, S., Sridhar, P., Smith, M., & Rauleder, J. (2024). Experimental and computational investigations of propeller-wing interactions. Proceedings of the Vertical Flight Society 80th Annual Forum, 1–27. https://doi.org/10.4050/f-0080-2024-1337

Tran, S. A., & Yeo, H. (2023). Transient and quasi-steady Numerical Simulations of tiltrotor conversion maneuvers. *Journal of the American Helicopter Society*, *68*(2), 18–32. https://doi.org/10.4050/jahs.68.022003

Turhan, B., Jawahar, H. K., Gautam, A., Syed, S., Vakil, G., Rezgui, D., & Azarpeyvand, M. (2024). Acoustic characteristics of phase-synchronized adjacent propellers. The Journal of the Acoustical Society of America, 155(5), 3242–3253. https://doi.org/10.1121/10.0025990

Walvekar, O., & Chakravarthy, S. (2023). An unsteady Reynolds–averaged Navier–Stokes–Large Eddy Simulation study of propeller–airframe interaction in distributed electric propulsion. Aerospace, 11(1), 17. https://doi.org/10.3390/aerospace11010017

Zhang, X., Zhang, W., Li, W., Zhang, X., & Lei, T. (2023). Experimental research on aero propulsion coupling characteristics of a distributed electric propulsion aircraft. Chinese Journal of Aeronautics, 36(2), 201–212. https://doi.org/10.1016/j.cja.2022.07.024